

A New Methodology for Dynamic Performance Simulation of a New Linear Switched Reluctance Motor based on Geometrical Dimensions

D.S.B. FONSECA

C.P. CABRITA

M.R.A. CALADO

Department of Electromechanical Engineering, CASE-Research Unit on Electrical Drives and Systems
 University of Beira Interior
 Calçada Fonte do Lameiro, P-6201-001 Covilhã
 PORTUGAL

Abstract: - The purpose of this paper is the simulation of the dynamic behavior of a Linear Switched Reluctance Machine (LSRM) taking into account the magnetic circuit saturation. The proposed methodology is based on the knowledge of the magnetization curves for one machine phase. This paper gives three possible ways to obtain the magnetization curves, and uses the fast one of them applied to a LSRM with a new topology. The other phase curves will be obtained considering symmetry and electromagnetic independency between phases.

Key-Words: - Linear Switched Reluctance Machines, performance simulation.

LIST OF SYMBOLS

b_p	Primary tooth length	w	Primary and secondary stack iron width
b_s	Secondary tooth length	$W_m(x_J, \psi_J)$	Stored magnetic energy
D_{cu}	Winding wire diameter	x	Machine position considering the origin on one unaligned position of phase 1
f_J	Phase J developed force	x_J	Phase relative position
F_R	Rated force	τ_p	Primary pole pitch
F_{pu}	Per unit average force considering F_R as base value	τ_s	Secondary pole pitch
f_{RES}	Load resistant force	Ψ_J	Flux linkage of a phase J
g	Airgap length	η	Expected efficiency
h_b	Coil length	B	Magnetic flux density
h_p	Primary slot depth	H	Magnetic field intensity
h_s	Secondary tooth depth	t	Time
$i_J(x_J, \psi_J)$	Phase instantaneous current	μ_0	Free space magnetic permeability
I_{max}	Maximum rms value of the coil current	M	Mass of the movable part
I_{pu}	Per unit rms current considering I_{max} value for base value	Int	Function that returns the integer part of a decimal number
J	Numerical index of one primary phase		
l_b	Coil width		
m	Primary phase number		
N	Number of turns per primary phase		
N_2	Secondary pole number		
N_{br}	Number of coils per winding parallel path		
N_e	Number of turns per primary coil		
N_r	Number of parallel paths of each primary phase		
R	Coil resistance value		
U_0	DC input voltage of power electronic converter		
u_J	Applied voltage to the phase J		
v	Machine linear speed		
v_R	Continuous rating linear speed		

1 Introduction

Switched reluctance machine dynamic simulation is now, as in the past, a concerning subject for its control development. Many of the known techniques are greatly simplified by assuming unsaturated machines, on the other hand accurate methodologies based on finite element analysis (FEA) requiring the use of expensive software and demands for large computation times.

It is the purpose of this work to present a new methodology for the LSRM performance evaluation. This methodology is based on the application of the 4th order Runge-Kutta method to the $(m+2)$ differential equation system.

2 Machine structure

Fig. 1 shows the topology of the machine used to exemplify the presented simulation methodology, and Table I present its dimensions. As can be seen, the LSRM presents a cheap secondary and modular primary construction. On the other hand, this topology increases significantly the electric, magnetic, thermal and physical independency between phases. Thus, mutual inductances between phases may be neglected without loss of accuracy.

3 Simulation methodology

For machine simulation one considers that all phase coils are series-connected, and the DC input voltage for power electronic energy converter is given by the following equation:

$$U = N_r U_0 \quad (1)$$

Independently of the chosen inverter topology, by application of the 2nd Kirchhoff's law one obtains the following time dependent equation for an excited phase circuit:

$$u_J(t) = R_J i_J(t) + \frac{\partial \Psi_J(t)}{\partial t} \quad (2)$$

where J is a natural number between 1 and m , and represents the phase index, and R_J is the equivalent phase resistance given by:

$$R_J = N_r N_{br} R \quad (3)$$

Table 1
Summary of the LSRM dimensions.

F_R [N]	100	g [mm]	3	h_s [mm]	42
v_R [m/s]	0,5	b_p [mm]	18	N_e	28319
M	4	b_s [mm]	18	l_b [mm]	45
U_0 [V]	200	τ_p [mm]	132	h_b [mm]	50
N_r	2	τ_s [mm]	48	D_{cu} [mm]	0,2
N_{br}	1	w [mm]	33	I_{max} [A]	0,11
N_2	6	h_p [mm]	50	R [Ω]	68.57

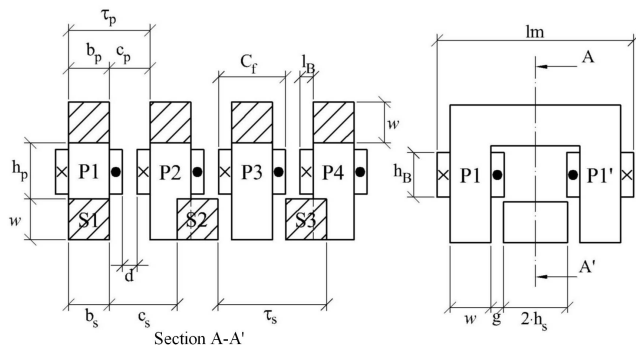


Fig.1 4-phase 8/6 Linear Switched Reluctance Machine geometry and envelope dimensions.

Alternatively, (2) can be rewritten to give the rate of change of flux linkage by phase J at instant t :

$$\frac{\partial \Psi_J(t)}{\partial t} = u_J(t) - R_J i_J(t) \quad (4)$$

Equation (4) represents m of the $(m+2)$ differential equations of the system. The remaining differential equations are related with the mechanical balance. Thus, by Newton's law:

$$\frac{\partial v(t)}{\partial t} = \frac{\left(\sum_{J=1}^m f_J(x, \Psi_J) \right) - f_{RES}(t)}{M} \quad (5)$$

$$\frac{\partial x(t)}{\partial t} = v(t) \quad (6)$$

where f_J is the developed force by phase J and $f_{res}(t)$ the resistant force or load force (as a result of all other forces, to be considered positive if they have the opposite direction of the speed).

Thus, knowing position, speed, and each phase flux linkage value in a time instant t_i , and applying the Runge-Kutta method to (4), (5) and (6) differential equations, considering a time step of Δt , one obtains respectively:

$$\Psi_J(t_i + \Delta t) = \Psi_J(t_i) \frac{K_{1\Psi J} + 2K_{2\Psi J} + 2K_{3\Psi J} + K_{4\Psi J}}{6} \quad (7)$$

$$v(t_i + \Delta t) = v(t_i) \frac{K_{1v} + 2K_{2v} + 2K_{3v} + K_{4v}}{6} \quad (8)$$

$$x(t_i + \Delta t) = x(t_i) \frac{K_{1x} + 2K_{2x} + 2K_{3x} + K_{4x}}{6} \quad (9)$$

where the K factors are obtained as follows:

$$K_{1\Psi J} = [u_J(t_i) - R_J i_J(x(t_i), \Psi_J(t_i))] \Delta t \quad (10)$$

$$K_{1v} = \frac{\left(\sum_{J=1}^m f_J(x(t_i), \Psi_J(t_i)) \right) - f_{RES}(t_i)}{M} \Delta t \quad (11)$$

$$K_{1x} = v(t_i) \Delta t \quad (12)$$

$$K_{2\Psi J} = \left[-R_J i_J \left[\left(x(t_i) + \frac{K_{1x}}{2} \right), \left(\Psi_J(t_i) + \frac{K_{1\Psi J}}{2} \right) \right] + u_J \left(t_i + \frac{\Delta t}{2} \right) \right] \Delta t \quad (13)$$

$$K_{2v} = \frac{\left(\sum_{J=1}^m f_J \left[\left(x(t_i) + \frac{K_{1x}}{2} \right), \left(\Psi_J(t_i) + \frac{K_{1\Psi J}}{2} \right) \right] \right) - f_{RES} \left(t_i + \frac{\Delta t}{2} \right)}{M} \Delta t \quad (14)$$

$$K_{2x} = \left[v(t_i) + \frac{K_{1v}}{2} \right] \Delta t \quad (15)$$

$$K_{3\psi J} = \left[-R_J i_J \left[\left(x(t_i) + \frac{K_{2x}}{2} \right), \left(\psi_J(t_i) + \frac{K_{2\psi J}}{2} \right) \right] + u_J \left(t_i + \frac{\Delta t}{2} \right) \right] \Delta t \quad (16)$$

$$K_{3v} = \frac{\left(\sum_{J=1}^m f_J \left[\left(x(t_i) + \frac{K_{2x}}{2} \right), \left(\psi_J(t_i) + \frac{K_{2\psi J}}{2} \right) \right] \right)}{M} - \frac{f_{RES} \left(t_i + \frac{\Delta t}{2} \right)}{M} \Delta t \quad (17)$$

$$K_{3x} = \left[v(t_i) + \frac{K_{2v}}{2} \right] \Delta t \quad (18)$$

$$K_{4\psi J} = \left[-R_J i_J \left[\left(x(t_i) + K_{3x} \right), \left(\psi_J(t_i) + K_{3\psi J} \right) \right] + u_J(t_i + \Delta t) \right] \Delta t \quad (19)$$

$$K_{4v} = \frac{\left(\sum_{J=1}^m f_J \left[\left(x(t_i) + K_{3x} \right), \left(\psi_J(t_i) + K_{3\psi J} \right) \right] \right)}{M} - \frac{f_{RES}(t_i + \Delta t)}{M} \Delta t \quad (20)$$

$$K_{4x} = \left[v(t_i) + K_{3v} \right] \Delta t \quad (21)$$

As can be seen, several values for current $I(x, \psi)$ and force $f(x, \psi)$ are necessary and are obtained by using the magnetization curves lookup table.

4 Magnetization curves

As explained, this simulation method requires the use of a lookup table representative of the magnetization curves.

For exact determination of the machine magnetization curves from dimensions there are two possible ways:

- from finite element analysis
- from static test measurements [1]

In this work the used methodology to obtain the magnetization curves is presented in [2,3] and is made through the linearization of the airgap length mean value between the unaligned and aligned positions.

According to [2] and considering all series-connected phase coils, the following equations represent a simplest and fast method to obtain ψ from B - H characteristic represented in Fig. 2:

$$\psi = N B w b_p \quad (22)$$

where N is the number of turns per phase, given by:

$$N = N_r N_{br} N_e \quad (23)$$

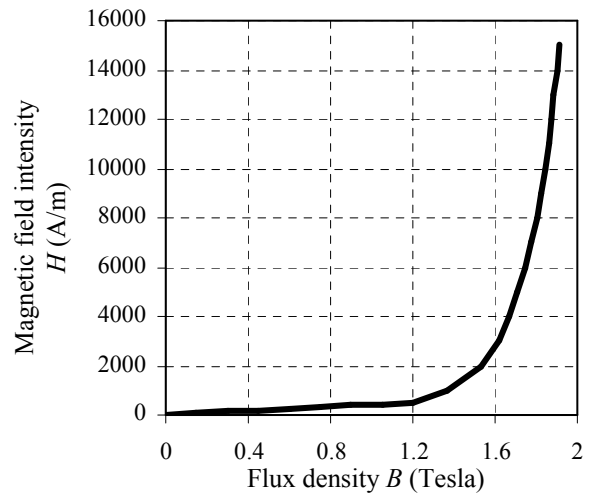


Fig.2 Magnetization curves for the magnetic circuit material.

Then, the input coil current for each relative position is obtained by using the following equation:

$$I(x, \psi) = \frac{H l_f(x) + \frac{\psi l_g(x)}{N w b_p \mu_0}}{N} \quad (24)$$

where l_g and l_f are respectively the airgap and iron average lengths of flux path, for each position.

Assuming $x=0$ for the unaligned position and for $0 < x < 0.5\tau_s$, l_g and l_f are given respectively by the following equations:

$$l_g(x) = 2(g + h_s) - \frac{4h_s x}{\tau_s} \quad (25)$$

$$l_f(x) = 2(h_p + 2(g + h_s + w)) - l_g(x) \quad (26)$$

Fig. 3 illustrates the airgap average length of flux path versus relative position characteristic. Note that both $x = 0$ and $x = \tau_s$ are unaligned positions, whereas $x = 0.5\tau_s$ is the aligned position.

Fig. 4 shows the magnetization characteristics of the machine phases. Note that for each position it is necessary to calculate the relative position of each phase considering the following relationship:

$$x_J(t_i) = \left(x(t_i) - \frac{J-1}{m} \tau_s \right) - \tau_s \cdot \text{Int} \left\{ \frac{x(t_i)}{\tau_s} - \frac{J-1}{m} \right\} \quad (27)$$

where x_J is the relative position of the phase J and Int function returns the integer part of a decimal number.

As can be seen, the lookup table values of the magnetization characteristics are stored in the form of necessary current in a phase to achieve a specific value of linkage flux in a given relative phase position.

Airgap average length of flux path versus relative position characteristic

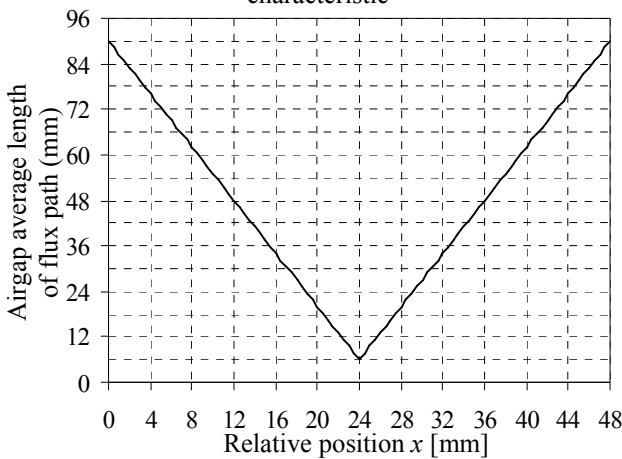


Fig.3 Airgap average length versus relative position.

Graphic representation of the machine magnetization curves lookup table

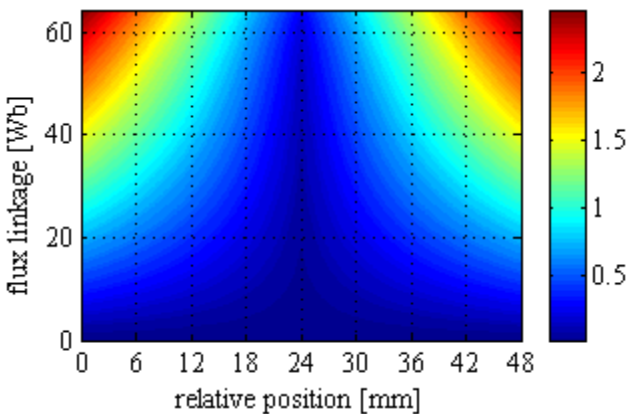


Fig.4 Phase current [A] versus relative position and flux linkage (magnetization curves).

5 Lookup table based calculations

There are three machine quantities stored in and extracted from lookup tables, phase current, stored magnetic energy and developed force. Thus, the necessary values obtained directly from a lookup table, are obtained from numerical interpolation using Cubic Spline Interpolation.

As well know, the computation time required for Cubic Spline Interpolation is directly related with the dimension of the data table. Thus, two different dimensions of the lookup tables are considered to analyze their dimension influence in the results.

5.1 Force calculation

The force calculation requires a more careful approach. Thus, taking into account that the exposed method uses both the flux linkage and relative

position as state variables, the developed force is derived from D’Lambert principle as follows [4]:

$$f_J(x_J, \psi_J) = - \left. \frac{\partial W_m(x, \psi)}{\partial x} \right|_{\psi=\psi_J} \quad (28)$$

$$f_J(x_J, \psi_J) = \frac{W_m[(x_J - \Delta x), \psi_J] - W_m[(x_J + \Delta x), \psi_J]}{2 \cdot \Delta x} \quad (29)$$

where Δx should tend to zero and must be lower than x_J , and W_m is the stored magnetic energy for one phase, and is represented by the following relationship:

$$W_m(x, \psi_J) = \int_{\psi=0}^{\psi=\psi_J} i(x, \psi) \partial \psi \Big|_{x=Const.} \quad (30)$$

At this point two possible ways can be adopted as follows:

Way No.1) To make a lookup table of stored magnetic energy, whose values are graphically presented in Fig. 5, and to use (29) during the simulation process. Concerning Fig. 5 one obtains the stored magnetic energy as a function of both relative position and flux linkage.

Way No.2) To use the stored magnetic energy lookup table to construct a lookup table of forces, like the one whose values are represented by Fig. 6, to be applied during the simulation process. In this lookup table, one obtains the developed force as a function of both relative position and flux linkage.

At first time the second way is more suitable to be used, however the force function presents a strong discontinuity for x_J equal to 0 and $0.5\tau_s$, where the force is equal to zero. That force discontinuity is directly related with the discontinuity of the derivative of I_g in order to x . Thus, some errors may be introduced by using the force lookup table around those positions.

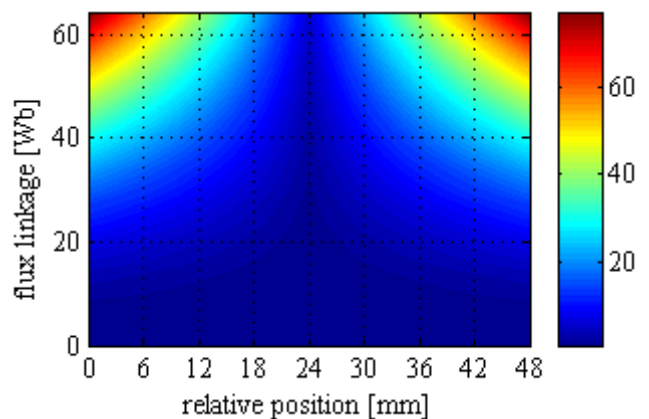


Fig.5 Stored magnetic energy [Joule] versus relative position and flux linkage, for one machine phase.

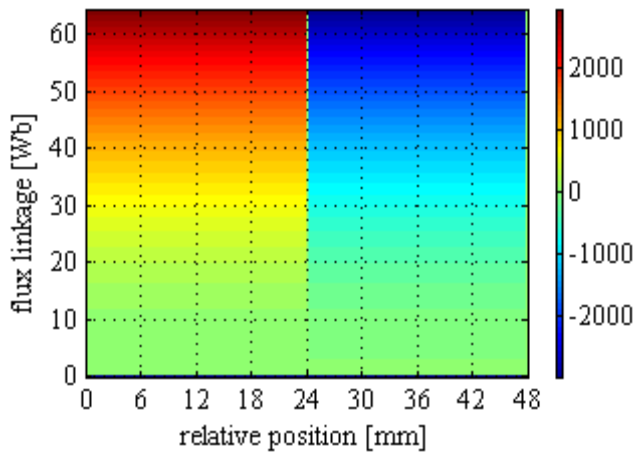


Fig.6 Phase developed force [N] versus relative position and flux linkage.

Note that for $0 < x_j < 0.5\tau_s$, due to the linearization of the airgap length mean value, the force value is only dependent from the linkage flux, remaining constant for all relative positions if the linkage flux remains constant. Note that constant flux in different positions implies different current values.

6 Results

In this work a 100 kg machine start up situation was considered. The simulation also considers a constant resistive force of 100N and the following control strategy:

- If $0 < x_j < 0.4\tau_s$ and $i_j \leq 0.24A$ then $u_j = U$.
- If $0 < x_j < 0.4\tau_s$ and $i_j \geq 0.25A$ then $u_j = -U$.
- If $0 < x_j < 0.4\tau_s$ and $0.24 < i_j < 0.25A$ then u_j remain constant.
- If $x_j \geq 0.4\tau_s$ and $i_j > 0$ then $u_j = -U$
- If $x_j \geq 0.4\tau_s$ and $i_j \leq 0$ then phase J is open
- If $x_j \leq 0$ then phase J is open.

As well known the maximum error of the Runge-Kutta method is equal to $(\Delta t)^4$, but in this case some errors can be introduced in the interpolation processes. Thus, the lookup table dimension, in terms of expressed values for each (x, ψ) pair, have a significant influence in the simulation accuracy.

In this work one set of lookup tables with 15 ψ values and 500 x values, and one set of lookup tables with 15 ψ values and 2000 x values was considered.

In Fig. 7 one can observe the influence of the lookup tables dimensions and force calculation methodology respectively on speed and developed force estimation.

As can be seen, there are no significant differences between the characteristics. A more careful and zoomed observation detects that:

- Both characteristics A) and C) have equal values.

- All characteristics are equal while the machine is stopped, because the only supplied phase is far away from both aligned and unaligned positions.
- Characteristic D) presents a smaller difference to A) and C) than B).

Considering this facts, and taking into account that A) and B) have a significantly lower computation time one will use configuration A) to observe the driver voltages and currents, as shown in Fig. 8.

7 Conclusions and future work

In authors' opinion, it can be concluded that the proposed and developed procedure, concerning the LSRM simulation, is a good method to be applied in the development way of the control algorithm.

As future work, the authors intend to:

- Search a more accurate function for the airgap average length characteristic.
- Extend this methodology to other LSRM topologies.

Acknowledgment

The authors would like to thank the financial support provided by the University of Beira Interior and the CASE-Centro de Accionamentos e Sistemas Eléctricos da Fundação para a Ciência e a Tecnologia (FCT) of Portugal.

References:

- [1] C. Cossar and T.J.E. Miller, Electromagnetic testing of switched reluctance motors, *ICEM'92*, September 14-17, 1992, pp. 470-474.
- [2] Fonseca, D. S. B., Cabrita, C. P., Calado, M. R. A. Linear Switched Reluctance Motor. A New Design Methodology Based on Performance Evaluation, *IEEE International Conference on Industrial Technology, Yasmine, Hammamet, Tunisia*, December 8-10, 2004, TF-001696.
- [3] D. S. B. Fonseca, C. P. Cabrita, M. R. A. Calado, Linear Switched Reluctance Motor. A new Topology for Fault Tolerant Traction Applications, *Proceedings of the 2005 IEEE International Electric Machines and Drives Conference, San Antonio, Texas, USA*, May 15-18, 2005, pp. 823-827.
- [4] Nicholas J. Nagel and Robert D. Lorenz, Modelling of a Saturated Switched-Reluctance Motor Using an Operating Point Analysis and the Unsaturated Torque Equation, *IEEE Trans. on Industry Applications*, Vol. 36, No. 3, May/June 2000, pp. 714-722.

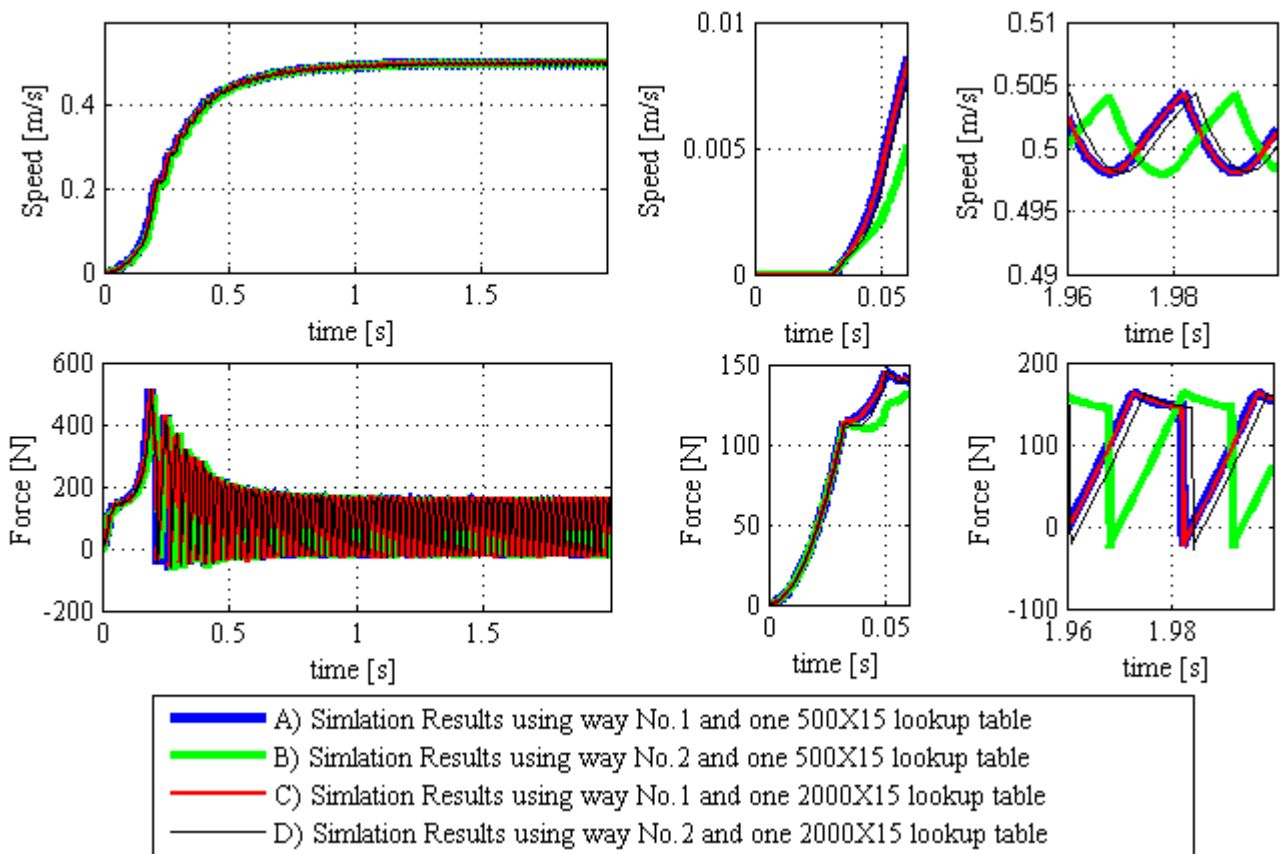


Fig.7 Machine expected output performance.

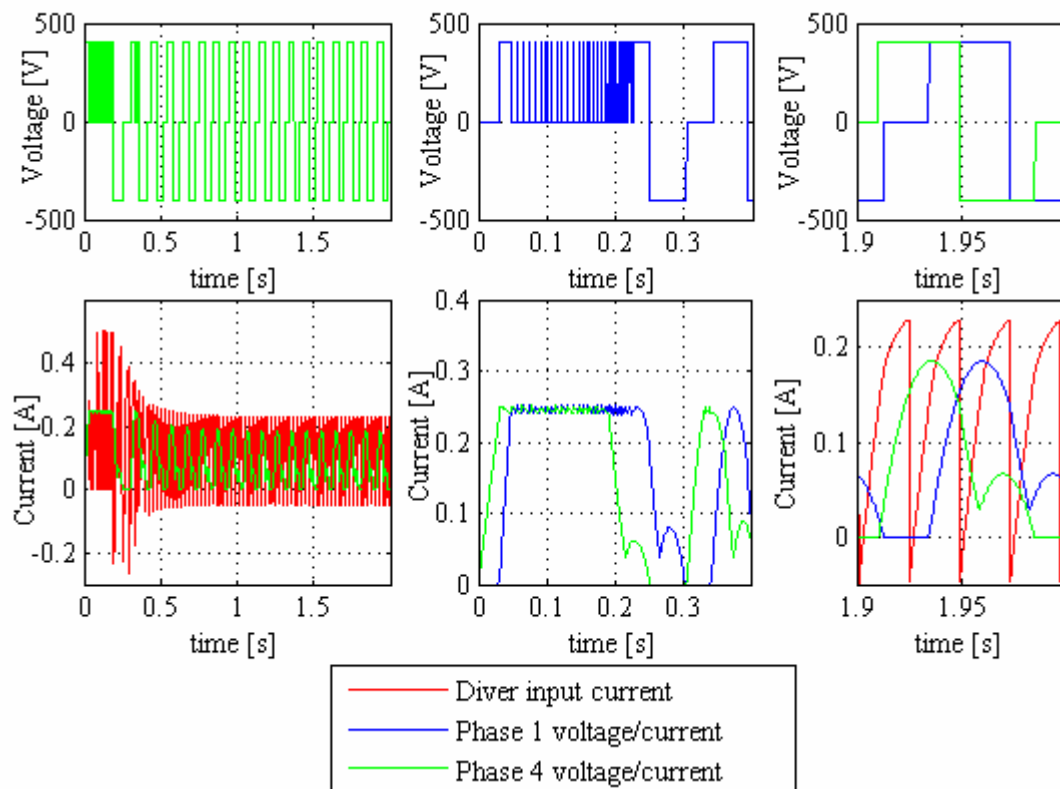


Fig.8 Machine expected input characteristics using Way No.1 and the 15X500 lookup tables.